Prospective Fault Currents in MVDC Distribution Grids – An Evaluation Methodology

Nils Langenberg[1,*], Marvin Bendig[1], Philipp Wienkamp[1], Andre Würde[1] and Albert Moser[1]
[1]IAEW at RWTH Aachen University, Aachen, Germany
*n.langenberg@iaew.rwth-aachen.de

Abstract

Medium Voltage Direct Current (MVDC) grids are becoming increasingly feasible for the realization of decentralized distribution applications for electrical energy. This is mainly due to cost reduction potential through advances in power electronic technologies as well as grid operation and service advantages with respect to the integration of renewable energy generation. However, the technological penetration of distribution grids on the basis of MVDC technologies is still hindered by a lack of standardization and operational experience. Key elements in this regard are suitable protection equipment and protection strategies. For the adequate design and development of such protection systems, knowledge on prospective fault currents in MVDC distribution grids is necessary. Within this paper an evaluation methodology is presented, which aims at a comparable evaluation of prospective fault currents in diverse MVDC grids by introducing comparable fault current characteristic values. On the basis of these values, the derivation of a current envelope curve is proposed. To demonstrate the applicability of the evaluation methodology, exemplary investigations of fault currents in a simulation test grid are conducted.

Keywords *– DC Distribution Grids, DC Fault Currents, Prospective Fault Currents, Operation of DC Grids*

1 Introduction

Increasing shares of distributed electrical energy generation in combination with a rising quantity of DC loads, such as industrial loads, data centres or large charging stations for electric vehicles, result in a shift in generation and load areas. The associated challenges, i.e. reverse power flow, require the expansion and reinforcement of conventional distribution grids [1, 2]. In this context, advances in efficiency and cost-effectiveness of voltage source converters (VSC) are leading to an increasing feasibility of Medium Voltage Direct Current applications on the distribution grid level [3, 4]. From an operative perspective, VSC-based MVDC distribution grids are enabling system operation and services such as flexible power flow control and cost savings due to fewer necessary conversion stages and higher utilization of cables [1, 2, 5]. Inter alia for these reasons, the implementation of MVDC distribution grids to connect renewable energy generation plants as well as large DC loads with connected Alternating Current (AC) grids is recognized as a possible solution for future energy distribution tasks [1, 4, 6].

However, no standardization in combination with a lack of operative experience are still posing challenges with respect to investment, installation and commissioning of fully operative MVDC distribution grids. Especially with regards to multi-terminal DC grids, fault clearing has to be done on the DC side in order to avoid a complete de-energization of the DC grid. One of the key elements to ensure the successful penetration of MVDC technologies is therefore, the availability of reliable and efficient protection equipment such as DC circuit breakers [1, 6]. The development of MVDC circuit breakers requires the knowledge of prospective DC fault currents and the associated stresses on protection and system equipment during a short circuit current interruption. Characteristic DC short circuit currents are showing a steep initial rise of current with a high amplitude after only a few ms. In contrast to fault currents in conventional AC distribution grids, DC fault currents do not necessarily contain current zero crossings and are developing at a faster rate [4, 7, 8, 9]. These characteristics in combination with the goal to protect sensible converter and system equipment make the current interruption more demanding for DC circuit breakers compared to AC circuit breakers. Additionally, the actual course of prospective DC fault currents is highly dependent on various system parameters [4, 5, 7, 10]. These include, among others, converter technology and parameterization, grid topology and extension, short-circuit power of connected AC grids as well as the system voltage level. In order to design adequate protection equipment, it is therefore necessary to investigate the influence of the DC grid architecture on prospective fault currents in MVDC distribution grids.

This paper aims at the derivation of an evaluation and analysis methodology of prospective fault currents in future MVDC grids. In combination with the knowledge of individual boundary parameters for different MVDC grids, requirements on novel MVDC protection equipment can be derived. The presentation of characteristic values of prospective MVDC fault currents is at the centre of this paper. To achieve a comparability, the introduction of the approach of current envelope curves for different fault case scenarios is aspired. In order to verify the evaluation method, a simulative representation of a MVDC test grid is developed. First exemplary findings on prospective DC fault currents and the applicability of the proposed evaluation methodology are shown.

2 Prospective DC Fault Currents

Adequate protection devices and strategies can be developed with the knowledge of stresses on grid components as a result of prospective DC fault currents in fault case scenarios. In this context, prospective fault currents are defined as being the current that would be flowing without any protective measures, such as fault current limiting devices or short circuit interruption processes. When considering the development of fault currents, generally three different stages can be identified, where the stages are distinguished by the respective source of fault feed-in. A simplified schematic representation of such a prospective fault current curve is depicted in **Figure 1**.

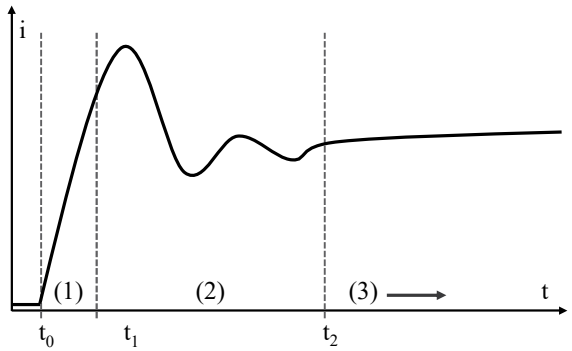

Figure 1 Simplified representation of a fault current curve in MVDC systems without fault limiting measures [11]

Within the first time period after the fault inception (1) at $t = t_0$, the fault current is solely fed by a discharge of the DC-side converter and filter capacitances. Since future MVDC grids will not necessarily have current limiting devices installed, the initial rate of rise is only limited by the fault impedance and the equivalent system inductance (cf. **Equation 1**) [5, 7, 8].

$$\frac{di_{Fault}}{dt} = \frac{U_{DC} - R_{Fault} \cdot i_{Fault}}{L_{System}} \quad (1)$$

The voltage drop on the affected line as a result of the low-impedance fault leads to an increase of current supply by the converter control. This in turn entails the beginning of compensation and superposition processes at $t > t_1$, in which the continuing discharge of capacitances is superimposed with an uncontrolled infeed from connected grids through the blocking converter modules (2) [4, 10]. Furthermore, although the extension of multi-terminal MVDC grids is envisioned to be comparatively small, traveling wave phenomena and delayed contribution from more distant converters need to be taken into account in this phase of fault current development. These superposition processes mark the second phase and are generally highly dependent on grid structure and the considered converter technology. In this regard, converters with fault current limiting capabilities, i.e. Modular Multilevel Converters (MMC) with full-bridge submodule configuration, can limit the fault current through active converter control [3]. After the capacitance discharge and compensation processes have subsided at $t > t_2$, a quasi-stationary state is reached in the third phase (3). In this state, the converter control is blocking the converter's power electronic switching devices in order to protect these from thermal and mechanical failures. As a result, the converter is functioning as an uncontrolled diode rectifier and the connected grid is feeding the fault current through the freewheeling diodes of the converter. The amplitude of the quasi-stationary fault current is limited only by the short-circuit power of the connected AC grids and the equivalent system impedance consisting of converter and transformer impedances and the line impedance from the point of common coupling (PCC) to the fault [7].

In a general conclusion of characteristic properties of prospective DC fault currents, a high initial rate of rise resulting in a high impulse current amplitude after only a few ms can be identified. Furthermore, DC fault currents do not necessarily contain current zero crossing and, if not interrupted, are showing quasi-stationary behaviour after the initial transient phases [4, 5, 12].

3 Evaluation Methodology

In order to provide a comparable evaluation and analysis methodology that is additionally adaptable to the individual case under consideration, characteristic values of fault current courses are presented. With this approach, the aforementioned dependencies of the actual fault current development in different system architectures can be investigated and the analysis as well as the comparison of various fault case scenarios are enabled.

3.1 Fault Current Characteristic Values

To highlight the characteristic values of fault current developments, the simplified representation from **Figure 1** is extended by an indication of the proposed characteristic values. The resulting featured fault current curve is depicted in **Figure 2**.

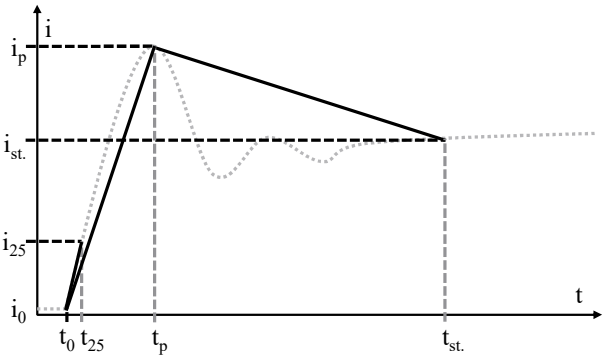

Figure 2 Schematic of characteristic fault current values in MVDC grids

A general classification into three categories can be identified and is indicated in **Figure 2**. Accordingly: Fault current amplitude specific values (dashed black), time specific values (dashed grey) and rate of rise or fall specific values (continuous black). An overview of the respective parameters is given in **Table 1**.

Table 1 Evaluation values for prospective fault currents in MVDC grids

Symbol	Parameter
i_p	Peak value of prospective fault current
$i_{st.}$	Medium value of quasi-stationary current
i_{25}	25%-value of peak value of prospective fault current
t_p	Time of peak value of prospective fault current
$t_{st.}$	Time of quasi-stationary value of prospective fault current
t_{25}	Time of 25%-value of peak value of prospective fault current
di_p/dt_p	Medium rate of rise from fault inception to peak value
$di_{st.}/dt_{st.}$	Medium rate of fall from peak value to quasi-stationary value
di_{25}/dt_{25}	Medium rate of rise from fault inception to 25%-value
Θ_1	Ratio of di_{25}/dt_{25} and di_p/dt_p
Θ_2	Ratio of $i_{st.}$ normalized to i_p

For the comparable evaluation of absolute current magnitudes, three values are differentiated. The peak value of the prospective fault current i_p represents the maximum amplitude of the impulse current. Similarly, the value of the mean quasi-stationary current $i_{st.}$ is defined as the mean value of the current after the second phase of the current development is completed. For this purpose, the quasi-stationary state is defined as the time, where the oscillation has decreased to within a 10 %-tolerance band. The use of this tolerance band provides for a definable beginning of the quasi-stationary state, since even in this phase oscillations due to the diode-rectifier characteristics are observable. In order to protect sensible converter station equipment, mainly power electronics, it is imperative to interrupt the short circuit current as quickly as possible. A time from fault inception to detection and subsequent fault clearing of only a few ms is identified [12, 13]. Therefore, a virtual characteristic value, i_{25}, is introduced that represents the 25 %-value of the peak value. This representation allows for a more accurate analysis of the stresses on DC switching equipment regarding absolute current and initial rate of rise of the fault current within the first phase of the current development. However, it is important to note, that an integrated analysis of the entire fault scenario is necessary to cover i.e. delayed short circuit detection or interruption processes.

Analogous to the previously described approach, the timing characteristics are derived to be the point in time, where the respective current magnitude is reached relative to the time of the fault inception (t_0). This means, that for i.e. t_p the time of the impulse current peak is considered. The beginning of the third phase, the quasi-stationary current, is marked by $t_{st.}$ and the time when the 25 %-value i_{25} is reached will be represented by t_{25}.

With the knowledge of the absolute current values and the time specific values, the corresponding medium rates of rise respectively rate of fall can be calculated. With this factor, the steepness of the current slope can be identified and protection equipment can be designed accordingly. The medium rate of rise for the prospective fault current from fault inception to the peak impulse current amplitude is demonstrated in **Equation 2**.

$$di_p/dt_p = \frac{i_p - i_0}{t_p - t_0} \tag{2}$$

The medium rate of rise for the 25 %-value is calculated likewise. For the medium rate of fall $di_{st.}/dt_{st.}$ a similar approach is taken, however the starting point is not the fault inception but rather the peak value of the impulse current (cf. **Equation 3**).

$$di_{st.}/dt_{st.} = \frac{i_{st.} - i_p}{t_{st.} - t_p} \tag{3}$$

To supplement the aforementioned characteristics, two additional descriptive values are introduced to comparably analyse fault scenarios in various MVDC systems. With the ratios θ_1 and θ_2, a description of the system dynamic as well as the system stiffness is enabled. The ratio Θ_1 is calculated according to **Equation 4** and can be interpreted as a representation of the impact of compensation processes on the actual fault current curve. A large Θ_1 is directly corresponding to a delayed absolute current peak and can in addition represent a relatively large spatial extension of the connected DC grid infrastructure. This can be attributed to the damping of current surges on lines through line impedances, which can lead to a contribution starting at a point in time, where the discharge of the DC side capacitances of the closest converter has already started to subside or the converter is already in blocking mode. In these cases, the resulting current curve can show a declining rate of rise before the contributions from more distant sources lead to a renewed increase of the rate of rise. If this is not taken into account, there is a risk of an underestimation of the stresses on electrical equipment which can be evaluated using Θ_1.

$$\Theta_1 = \frac{di_{25}/dt_{25}}{di_p/dt_p} \tag{4}$$

The second considered ratio to be introduced is Θ_2. This value describes the value of the quasi-stationary current $i_{st.}$ normalized to the absolute current amplitude i_p. The according calculation can be obtained from **Equation 5**.

$$\Theta_2 = \frac{i_{st.}}{i_p} \tag{5}$$

This ratio allows for the interpretation of the short circuit power of the connected AC grids and can be used in order to design adequate protection equipment. $\Theta_2 = 1$ means, that the quasi-stationary current $i_{st.}$ is of the same amplitude as the impulse current i_p. This means, that the influence of the DC side capacitances as well as the converter power on the course of the fault current is comparably low. A relatively low value of Θ_2 however indicates a comparatively large overshoot of the impulse current i_p as compared to the quasi-stationary current amplitude $i_{st.}$. This in turn could be used in the design of protection systematics, where one possible concept could be to endure the high impulse current and interrupt the fault current in the third phase.

3.2 Fault Current Envelope Curve

Since MVDC applications are subject to a high cost pressure due to the need to compete with conventional AC distribution grids, it is not desirable to develop MVDC protection equipment individually for specific use cases. Rather it is advisable, to develop solutions that can be utilized in numerous applications. With regards to development and testing of conventional AC switching equipment, a similar challenge is posed by various transient recovery voltage (TRV) curves. In this case, a proven practice has been to define TRV envelope curves as testing requirements for new components in order to ensure the functionality and safety of new assets [14]. The rationale behind this procedure is that if, i.e. a circuit breaker can handle the stresses posed by the envelope curve, the safe functionality can be expected in grid applications which are included in the envelope curve [14]. A similar approach is proposed in this paper, where the results from grid simulations as well as future field measurements can be used to derive current envelope curves. For this, the resulting prospective fault currents are to be investigated according to the aforementioned characteristic values. On the basis of these values, current envelope curves can be defined, which allow for the adequate representation of the underlying simulative analyses.

This being said, since the influences of different system design aspects have been proven to be non-negligible, the derivation of a singular current envelope curve is expected to not be possible [4,5,7]. For this reason, it is proposed to define different current envelope curves for different fault case scenarios depending on, among others, grid topology, converter technology, fault impedance as well as number of points of common coupling and the respective connected grids and loads. The approach of different yet synoptic current envelope curves limits the amount of diversity to be considered since related fault case scenarios can be summarized within one current envelope curve. Furthermore, the proposed approach allows for standardization with regards to development and testing of future MVDC switching equipment.

4 Simulative Investigation

4.1 Test Grid Model

To demonstrate the proposed evaluation methodology, exemplary grid simulations using the EMT software PLECS are conducted. For the investigation of the influence of various system parameters, a simulation model of a test grid is developed. The considered test grid consists of five converter stations with the respective points of common coupling (PCC_1 - PCC_5) to the according AC grids. The analysis of the grid topology's influence on prospective DC fault currents is chosen as a representative analysis and therefore, converter stations, connected underlying AC grids and the cable parameters are unified. These exemplary simulations are considered for the demonstration of the applicability of the evaluation method and do not claim to be a complete representation of the influence of different parameters on the fault current development.

As the representation of the investigated simulation model in **Figure 3** shows, the grid topology is varied between radial, ring and meshed topology. To eliminate the influence of the cable length, the distance between the converter stations is kept constant for all considered grid topologies. The distance between PCC_1, PCC_2 and PCC_3 as well as between PCC_4 and PCC_5, is held constant at $l_1 = 10\ km$. The connection between PCC_5 with PCC_1 and PCC_2 as well as the connection from PCC_4 to PCC_1, PCC_2 and PCC_3 is set to $l_2 = 15\ km$.

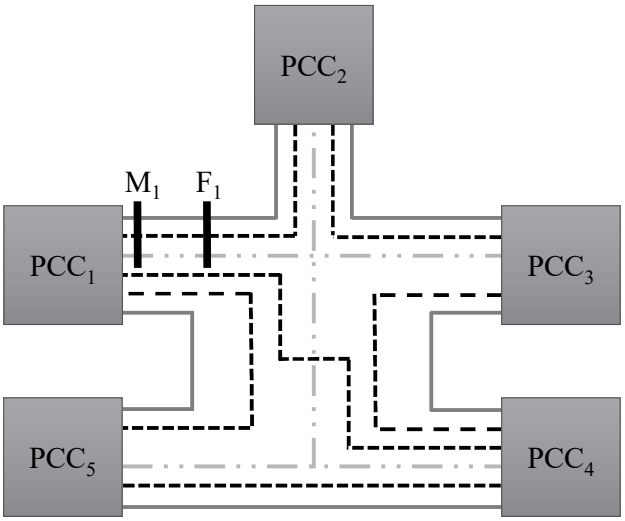

Figure 3 MVDC grid model in ring (continuous grey), radial (dashed grey) and meshed (dashed black) topology

The exemplary initialization of a short circuit fault is applied to the fault location F_1, on the cable connection between station PCC_1 and PCC_2 at a distance of 2.5 km from PCC_1 [11]. The equivalent position is highlighted in **Figure 3**. Similarly, the position of the considered current measurement is indicated at position M_1. This measurement is obtained at position M_1 in order to show the current stresses on a circuit breaker at the beginning of the faulty line as seen from station PPC_1. The simulation parameter overview can be acquired from **Table 2**.

Table 2 Parameters of the Simulation Model

	PCC_1 – PCC_5
Connected AC Grids	
Nominal Voltage	20 kV
Short Circuit Power	500 MVA
R/X-ratio	0.25
Frequency	50 Hz
Converter Stations	
Converter Topology	Two-Level VSC-Converter
Nominal Power	40 MW
Nominal DC Voltage	± 5 kV_{DC}
DC Capacitor	5mF
Line Parameters	
Resistance per unit length	24,7 mΩ/km
Inductivity per unit length	280 µH/km

4.2 Exemplary Results

An exemplary investigation is conducted to demonstrate the applicability of the proposed evaluation methodology as shown in chapter 3 with the results being depicted in **Figure 4**. The study object here is the influence of the grid topology on the prospective short circuit current that flows through the circuit breaker of the faulty cable connection.

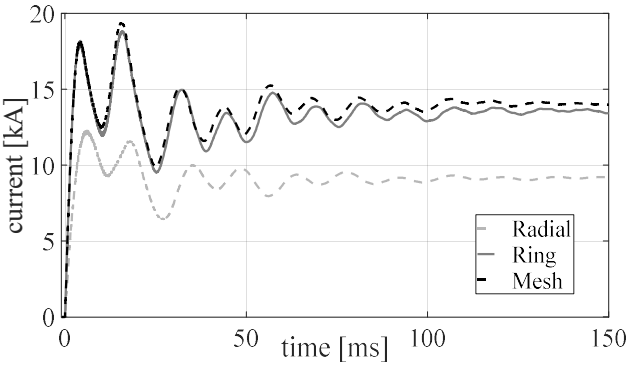

Figure 4 Simulated prospective short circuit fault currents in radial, ring and meshed grid topology

Results from all investigated grid topologies show a similar behaviour and can be explained with the characteristic fault current development, as described in chapter 2. The characteristic values are summarized in **Table 3**. From the positioning of the measurement M_1, it is obvious that the resulting impulse current $i_p = 12.32\ kA$ for the radial topology is comparably lower than in ring ($i_p = 18.83\ kA$) or in meshed ($i_p = 19.42\ kA$) topology. This is due to the fact, that in the latter two topologies, a common busbar is present, where the fault infeed from the other converter stations can be measured. Therefore, in these cases the circuit breaker at the converter station PCC_1 has to endure higher electrical stresses. The grid scenarios of the ring and meshed topology show the reason for the introduction of the virtual values of i_{25}, t_{25} and di_{25}/dt_{25}. Since the peak of the impulse current in these scenarios is only reached after a first curve dip due to compensation processes, the calculation of the absolute time to peak value is misleading. The associated rate of rise and therefore also the first, most demanding phase would be underestimated. This can be highlighted by the exemplary comparison of the mean rate of rises in the case of a ring grid topology. The mean rate of rise to the peak impulse current is calculated to $di_p/dt_p = 1.19\ kA/ms$, whereas the mean rate of rise to the 25 %-value is calculated to $di_{25}/dt_{25} = 7.72\ kA/ms$. This is also true for the case of the radial grid topology, even though the impulse current peak is reached before a first current curve dip ($di_p/dt_p = 2.03\ kA/ms$ as opposed to $di_{25}/dt_{25} = 4.75\ kA/ms$).

A case for the necessity of the proposed virtual values can also be made via consideration of the proposed ratios Θ_1 and Θ_2. An analysis of only the absolute values of the current amplitude as well as the mean rate of rises to the amplitude of the prospective fault current leads to a vast underestimation of the initial stresses. This can be proven through the values for Θ_1, where in the case of the considered radial grid a ratio $\Theta_1 = 2.34$ can be identified. This means, that the initial stresses are underestimated by more than double. Even greater is this underestimation effect for the ring ($\Theta_1 = 6.49$) as well as the meshed ($\Theta_1 = 6.27$) topologies. Based on the aforementioned observations, the characterization of fault currents through the proposed virtual value Θ_1 promises a more realistic representation.

Furthermore, through observation of Θ_2, it can be assumed, that the quasi-stationary values for all three considered fault case scenarios are within 75 % of the peak amplitude of the prospective fault current. Knowledge on the parameters Θ_1 and Θ_2 are especially important when considering development and testing aspects of future MVDC protection equipment.

Table 3 Investigation results for different MVDC grid topologies for considered parameterization

	Radial	**Ring**	**Meshed**
i_p	12.32 kA	18.83 kA	19.42 kA
$i_{st.}$	9.12 kA	13.55 kA	14.01 kA
i_{25}	3.08 kA	4.71 kA	4.86 kA
t_p	6.08 ms	15.86 ms	15.59 ms
$t_{st.}$	70.19 ms	82.09 ms	81.13 ms
t_{25}	0.80 ms	0.61 ms	0.62 ms
di_p/dt_p	2.03 kA/ms	1.19 kA/ms	1.25 kA/ms
$di_{st.}/dt_{st.}$	-0.050 kA/ms	-0.078 kA/ms	-0.083 kA/ms
di_{25}/dt_{25}	4.75 kA/ms	7.72 kA/ms	7.84 kA/ms
Θ_1	2.34	6.49	6.27
Θ_2	0.74	0.72	0.72

4.3 Exemplary Current Envelope Curve

As is described in chapter 3, the introduction of an envelope current curve is proposed as an addition to the virtual characteristic values. For this purpose, the totality of grid investigations is taken into account and an envelope curve is derived, which includes all characteristic parameters. For this paper, the shown results from grid simulations regarding the influence of grid topology design, as shown in **Figure 4**, are used to derive an exemplary envelope current curve. The resulting current curve is added to the schematic and can be obtained from **Figure 5**, where it is indicated by the continuous black line. The envelope curve is characterized by an initial rate of rise of $di_{25}/dt_{25} = 7.84\ kA/ms$ with a current peak at $i_p = 19.42\ kA$. The aspired quasi-stationary current is valued at $i_{st.} = 14.45\ kA$, resulting in $\Theta_2 = 0.74$.

It can be seen, that all simulated current curves are positioned within the envelope curve. The implied reason for this is the necessity for a generally applicable current curve as a basis for development and testing of novel MVDC switching equipment. However, as mentioned before, various current envelope curves for different system designs are to be derived. In the presented fault case scenarios, the envelope curve is dominated by characteristics obtained from the meshed grid topology. For an extensive sensitivity analysis, it is expected, that the resulting current envelope curves will be defined by various influencing parameters. This sensitivity analysis however, is not within the scope of this paper.

It is also important to note, that besides focusing on the investigation of prospective DC fault currents in MVDC grids, the voltage stresses on switching equipment need to be considered. Also these stresses are not within the scope of this paper.

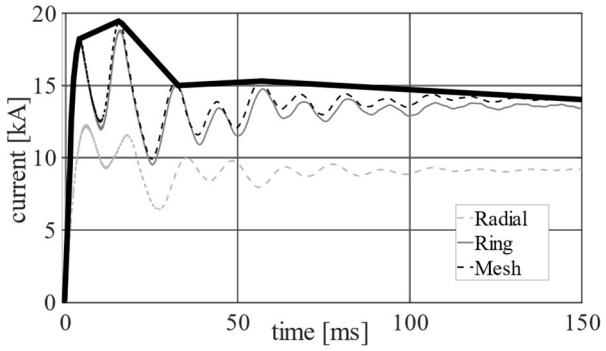

Figure 5 Exemplary current envelope curve (continuous black) on the basis of the considered fault case scenarios

5 Conclusion

Prospective fault currents are important aspects of consideration for the development and testing of MVDC protection equipment. This paper proposes a methodology to comparably evaluate different fault case scenarios and their impact on the fault current development. For this purpose, characteristic fault current values are introduced. In addition to absolute values, a virtual value is proposed for a better representation of stresses on equipment within the initial highly transient phase after the fault inception. Furthermore, the introduction of a current envelope curve to cover multiple fault case scenarios in one parameter for development and testing requirements is shown. The functionality of the proposed methodology is then demonstrated on the basis of exemplary grid investigations.

6 Acknowledgements

Funded by the Federal Ministry of Research and Education (BMBF, FKZ 03SF0595), Flexible Electrical Networks (FEN) Research Campus.

7 Literature

[1] Cigré WG C6.31: “Medium voltage direct current (MVDC) grid feasibility study”, Technical Brochure 793, Cigré, Paris, 2020

[2] Eissa, M. M.: “Medium-Voltage Direct Current Grid, Resilient Operation, Control and Protection”, Academic Press Inc, San Diego, 2019

[3] Fazel, S. S.: “Investigation and Comparison of Multi-Level Converters for Medium Voltage Applications”, Dissertation, TU Berlin, Berlin, 2007

[4] Stumpe, M., Tünnerhoff, P., Schnettler, A. and Schmidt, D.: “Grid Topology and technology influences on selective protection concepts for multi-terminal medium voltage DC grids”, The Journal of Engineering, Vol. 15, 2018, pp. 796-801

[5] Bleilevens, R., Priebe, J., Wehbring, N. and Moser, A.: “Identification of Relevant Fault Types for Grid Planning of Distribution Grids”, VDE Verlag GmbH, Berlin, 2018

[6] Lee, K., Ukil, A. and Yeap, Y.-M.: “Short-Circuit Protection for MV & LVDC Grid”, IEEE PES Asia-Pacific Power, Hong Kong, 2014

[7] Belda, N., Plets, C. and Smeets, R. P. P.: “Analysis of Faults in Multi-Terminal HVDC Grid for Definition of Test Requirements of HVDC Circuit Breakers”, IEEE Transactions on Power Delivery, 2017

[8] Cigré JWG A3/B4.34: “Technical Requirements and Specifications of State-Of-The-Art HVDC Switching Equipment”, Technical Brochure 683. Cigré, Paris, 2017

[9] Bucher, M. K.: “Comparison of Fault Currents in Multiterminal HVDC Grids with Different Grounding Schemes”, IEEE PES General Meeting, National Harbour, USA, 2014

[10] Wasserrab, A., Just, B. and Balzer, G.: “Contribution of HVDC Converters to the DC Circuit Current”, 48th International Universities’ Power, Dublin, 2013

[11] Bleilevens, R. and Moser, A.: “Identification of Required Converter Models for a Simplified Short Circuit Current Calculation of DC Distribution Grids”, 54th International Universities Power Engineering Conference, Bucharest, 2019

[12] Wang, T. and Monti, A.: “Fault Detection and Isolation in DC Microgrids Based on Singularity Detection in the Second Derivative of Local Current Measurement”, IEEE Journal of Emerging and Selected Topics in Power Electronics, New York, 2020

[13] Akhmatov, V., Callavik, M., Franck, C. M., Rye, S. E., Ahndorf, T., Bucher, M. K., Muller, H., Schettler, F. and Wiget, R.: “Technical Guidelines and Prestandardization Work for First HVDC Grids”, IEEE Transactions on Power Delivery, Vol 29, No. 1, 2014, pp.327-335

[14] DIN EN 62271-100: „High-voltage switchgear and controlgear – Part 100: Alternating-current circuit breakers“, in German: „Hochspannungsschaltgeräte und -Schaltanlagen – Teil 100: Wechselstrom-Leistungsschalter“, 2013